

PAPER • OPEN ACCESS

Observation of multiple rotons and multidirectional roton-like dispersion relations in acoustic metamaterials

To cite this article: Zhenxiao Zhu *et al* 2022 *New J. Phys.* **24** 123019

View the [article online](#) for updates and enhancements.

You may also like

- [Anisotropic reduced diffusion in dilute liquid \$^3\text{He}\$ - \$^4\text{He}\$ mixture in ordered aerogel](#)
K Safiullin, V Kuzmin, A Stanislavovas et al.
- [Excitations in the Yang–Gaudin Bose gas](#)
Neil J Robinson and Robert M Konik
- [Excitations in the quantum liquid \$^4\text{He}\$: A review](#)
H R Glyde



PAPER

Observation of multiple rotons and multidirectional roton-like dispersion relations in acoustic metamaterials

Zhenxiao Zhu^{1,5}, Zhen Gao^{1,5,*}, Gui-Geng Liu^{2,5}, Yong Ge³, Yin Wang³, Xiang Xi¹, Bei Yan¹, Fujia Chen⁴, Perry Ping Shum¹, Hong-xiang Sun^{3,*}  and Yihao Yang^{4,*}¹ Department of Electrical and Electronic Engineering, Southern University of Science and Technology, Shenzhen 518055, People's Republic of China² Division of Physics and Applied Physics, School of Physical and Mathematical Sciences, Nanyang Technological University, 21 Nanyang Link, Singapore 637371, Singapore³ School of Physics and Electronic Engineering, Jiangsu University, Zhenjiang 212013, People's Republic of China⁴ Interdisciplinary Center for Quantum Information, State Key Laboratory of Modern Optical Instrumentation, ZJU-Hangzhou Global Science and Technology Innovation Center, Zhejiang University, Hangzhou 310027, People's Republic of China⁵ These authors contributed equally to this work

* Authors to whom any correspondence should be addressed.

E-mail: gaoz@sustech.edu.cn, jsdxshx@ujs.edu.cn and yangyihao@zju.edu.cn**Keywords:** long-range interaction, roton-like dispersion, multiple rotons, multidirectional roton-like dispersion, nonlocal acoustic metamaterials

RECEIVED

4 April 2022

REVISED

22 November 2022

ACCEPTED FOR PUBLICATION

30 November 2022

PUBLISHED

15 December 2022

Original content from
this work may be used
under the terms of the
[Creative Commons
Attribution 4.0 licence](https://creativecommons.org/licenses/by/4.0/).Any further distribution
of this work must
maintain attribution to
the author(s) and the title
of the work, journal
citation and DOI.

Abstract

Roton dispersion relations were firstly predicted by Landau and have been extensively explored in correlated quantum systems at low temperatures. Recently, the roton-like dispersion relations were theoretically extended to classical acoustics, which, however, have remained elusive in reality. Here, we report the experimental observation of roton-like dispersions in acoustic metamaterials with beyond-nearest-neighbour interactions at ambient temperatures. The resulting metamaterial supports multiple coexisting modes with different wavevectors and group velocities at the same frequency and broadband backward waves, analogous to the ‘return flow’ termed by Feynman in the context of rotons. By increasing the order of long-range interaction, we observe multiple rotons on a single dispersion band, which have never appeared in Landau’s prediction or any other condensed-matter or classical-wave studies. Moreover, we have also theoretically proposed and experimentally observed multidirectional roton-like dispersion relations in a two-dimensional nonlocal acoustic metamaterial. The realization of roton-like dispersions in metamaterials could pave the way to explore novel physics and applications on quantum-inspired phenomena in classical systems.

1. Introduction

The concept of roton, an elementary excitation (quasiparticle), was firstly predicted by Landau [1] to explain the unusual thermodynamic properties of superfluid ⁴He, laying the foundation for the development of several areas of modern physics such as Bose–Einstein condensation, superfluidity, phase transition, and quantum field theory. In such condensates, the dispersion relation does not exhibit the usual monotonic growth of energy with momentum in gases, liquids, and solids. Instead, its dispersion relation evolves from linear at low momentum (phonon) to parabolic-like with a minimum (roton) at finite momentum. Following the suggestion by Richard Feynman [2, 3], inelastic neutron scattering experiment [4–7] fully confirmed Landau’s remarkable intuition. Later, roton-type collective modes have been widely discovered experimentally in different quantum systems at low temperatures, such as quantum spin liquid [8], fractional quantum Hall states [9], two-dimensional Fermi liquid [10], and quantum gas with cavity-mediated long-range interactions [11, 12].

Although undoubtedly that the rotons in superfluid are inherently quantum, their unique dispersion relations could in principle also be observed for classical waves such as elastic, acoustic, and electromagnetic

waves. One of the candidate platforms to realize the roton-like dispersion relations is acoustic metamaterial [13] that has been widely adopted to study a variety of unusual physic phenomena such as negative refraction [14–16], superlensing [17, 18], invisibility cloaking [19, 20] and topological protection [21–26]. Indeed, recent theoretical studies [27, 28] have suggested that the roton-like dispersion relations can be achieved in classical acoustic metamaterials by introducing beyond-nearest-neighbour interactions. The resulting roton-like dispersion relation has many intriguing features that could manipulate acoustic or electromagnetic waves beyond the standard negative refractive index metamaterials [29], such as broadband backwave propagation, multiple coexisting Bloch modes with different wavevectors at the same frequency, and a large density of states at the roton minimum and maxon maximum with zero group velocity (ZGV). However, the roton-like dispersion in classical-wave systems under ambient conditions has remained elusive to observation to date.

Here, by exploiting long-range interactions, we report the experimental observation of roton-like dispersion relations in nonlocal acoustic metamaterials for the first time. The fabricated acoustic metamaterial consists of cube resonators and two types of isolated connecting tubes, which play the roles of nearest-neighbour and beyond-nearest-neighbour interactions, respectively. Via direct acoustic measurements, we experimentally observe the roton-like dispersion relations in acoustic metamaterials, confirming Landau's prediction about the roton-like dispersion behaviours in a classical system. Moreover, by increasing the long-range interaction order, more slope inversions can be achieved in the first Brillouin zone, leading to multiple rotons in a single dispersion band, which have never been predicted or observed in any quantum system. We also discuss the impact of structural chirality on roton-like behaviour. Finally, we have theoretically proposed and experimentally realized multidirectional roton-like dispersions in a 2D nonlocal acoustic metamaterial.

2. Methods

2.1. Numerical simulations

All metamaterial full-wave simulations are performed in the pressure acoustic module of COMSOL Multiphysics. In all simulations, the background medium air is modelled with a density of 1.29 kg m^{-3} and a speed of sound of 340 m s^{-1} . The plastic stereolithography can be considered as a hard boundary during the simulations due to the substantial acoustic impedance contrast compared with air. For calculating the dispersion relations, periodic boundary conditions are set in the x -direction (1D) or both x - and y -directions (2D), and other boundaries are considered as hard acoustic boundaries. The dispersion slope (i.e. group velocity) is calculated by $v_g = d\omega/dk$, where ω is the angular frequency and k is wave vector in the momentum space.

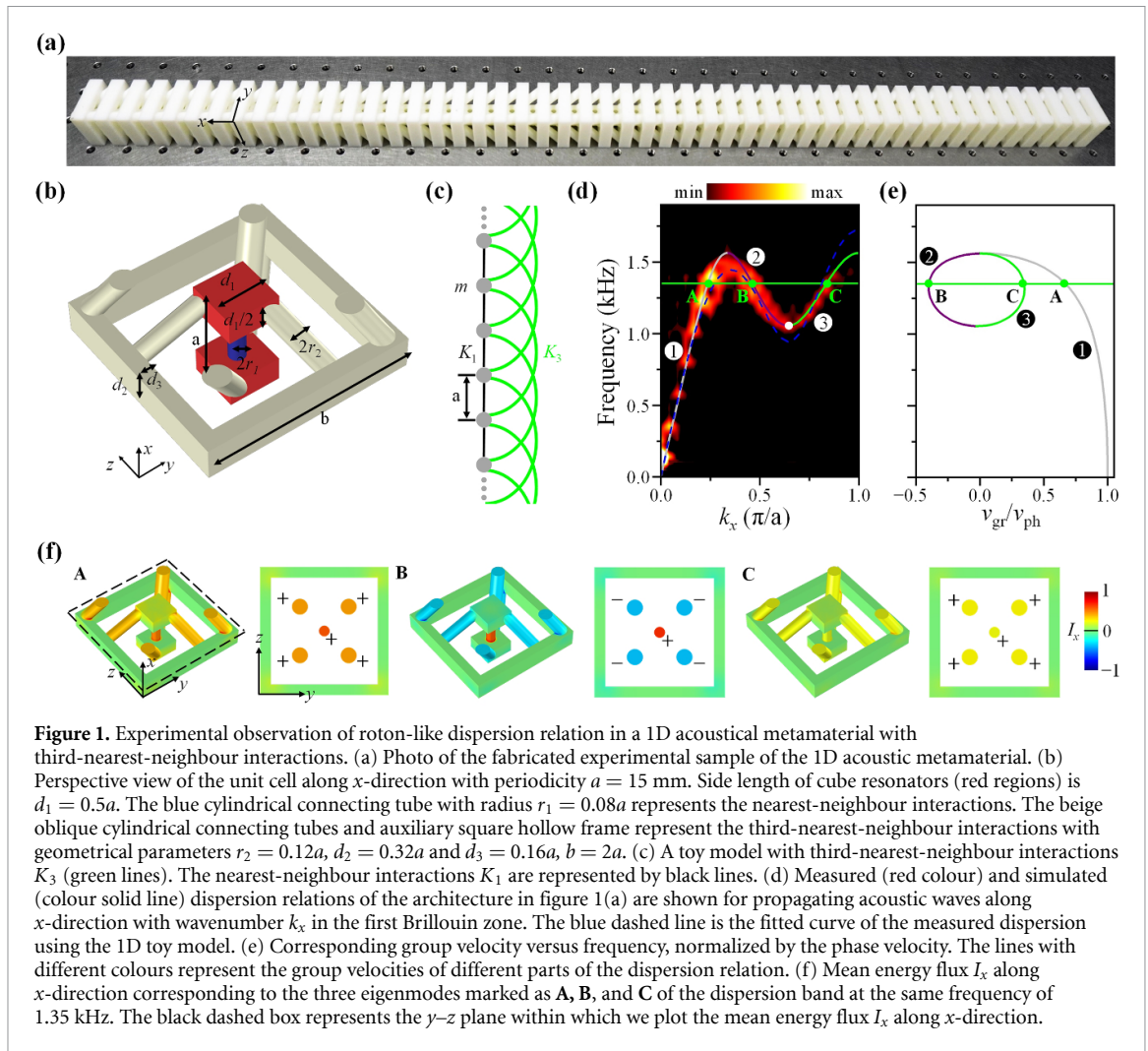
2.2. Experimental details

The samples are fabricated with an additive manufacturing technique (that is, stereolithography) with a resin of a thickness of 5 mm and 1×50 -unit cells stacked along the x -direction (1D) or 30×30 -unit cells stacked along both x - and y -direction (2D). The materials are photosensitive resin with a modulus of 2880 MPa and a density of 1.10 g cm^{-3} . The structures can be viewed as rigid walls for the acoustic waves that propagate in the acoustic metamaterials due to the large impedance mismatch between air and the material. A small hole ($r = 2 \text{ mm}$) is located on the centre of each cube resonator for excitation and detection. When not in use, they are blocked by plugs. In the experiment, a broadband sound signal is launched by a balanced armature speaker guided into the sample through a small hole on the centre of cube resonator to excite the acoustic modes. Another microphone (Brüel & Kjær Type 4961, of about 3.2 mm radius) in a sealed sleeve with a tube of 1 mm radius and 250 mm length is inserted into each cube resonator through the small hole to collect the acoustic signals one by one. The measured data is processed by a Brüel & Kjær 3160-A-022 module to extract the frequency spectrum with 2 Hz resolution. Spatial Fourier transforms are applied to the complex acoustic field distributions to obtain the measured dispersion relations.

3. Results

3.1. Observation of the roton-like dispersion relation in a nonlocal acoustic metamaterial

The three-dimensional (3D) experimental sample of the acoustic metamaterial with the roton-like dispersion relation is fabricated with stereolithography 3D printing technology, as shown in figure 1(a). It consists of 50 unit cells along x -direction. Each unit cell has a cube resonator with side length d_1 (see the red region of figure 1(b)). For the convenience of experimental measurement, each cube resonator has a small hole for detecting the acoustic waves in the resonator. These holes are sealed when not in use and have a negligible impact on the dispersion relation of the acoustic metamaterial. The vertical cylindrical tubes with



a radius of r_1 connecting two nearest-neighbour resonators serve as the nearest-neighbour interactions. The oblique cylindrical tubes with a radius of r_2 connecting two third-nearest-neighbour resonators serve as the beyond-nearest-neighbour interactions with an order of $N = 3$. The hollow frame with height d_2 serves as an auxiliary structure to mediate the third-nearest-neighbour interactions. The oblique cylindrical tubes connect to the auxiliary hollow frame, from which another set of oblique cylindrical tubes is connected to the third-nearest-neighbour of the starting cube resonator to trigger the long-range interaction. The cube resonators, cylindrical oblique tubes, and the auxiliary frames are filled with air and made of hard plastics to ensure that the inner surfaces meet the hard boundary condition. Besides, the acoustic metamaterial structure is achiral, which exhibits mirror symmetry and inversion symmetry.

In the experiments, the sound wave generated by a broadband speaker is guided into the waveguide through a small hole at the leftmost cube resonator. A microphone probe is inserted into the other holes at each cube resonator to measure the acoustic pressure signal. This measurement is repeated for all cube resonators of the sample one by one (see section 2). Note that all cylindrical holes are plugged except for the one that opens to measure the acoustic signal. After performing a 1D Fourier transform to the measured acoustic field distributions, we obtain the dispersion relations of the nonlocal acoustic metamaterials (see the colour plotted in figure 1(d)). One can clearly observe the pronounced roton-like dispersion relation—the dispersion band starts from zero frequency and zero momentum with linear growth at low wavevectors, then evolves continuously to reach a maximum, and the dispersion slope (i.e. group velocity $v_g = d\omega/dk$) reverses from positive to negative (see figure 1(e)), displaying a pronounced ‘roton’ minimum (white dot in figure 1(d)) before increasing again. The dispersion relation closely resembles the dispersion curve of the elementary excitations of a Bose superfluid predicted by Landau [1]. The experimental results agree with the simulated counterpart (see the colour curve in figure 1(d)) very well.

The roton-like dispersion relation has several intriguing features, which may find potential applications to manipulate acoustic waves in uncommon ways. First, the ‘maxon’ maximum and ‘roton’ minimum with ZGV produce singularities with an extremely high density of states that can be utilized to significantly

enhance the wave-matter interactions. Second, the negative slope of roton-like dispersion relation gives rise to broadband backward waves that could lead to acoustic negative refraction and superlensing [14–18] based on a new mechanism of nonlocal effect. Third, at a given frequency, the dispersion curve can support multiple coexisting Bloch modes with different wavevectors, phase velocities, and group velocities. Note that Lamb waves in natural materials also show ZGV modes [30, 31] and multiple coexisting modes at a given frequency. However, the dispersion curves of Lamb waves are entirely different from the roton-like dispersion relation. The unique dispersion curve of superfluid comes from the interplay between phonons and rotons. Therefore, for the roton-like dispersion, the dispersion relation starts from a linear growth (corresponding to low-energy phonons); at a certain large momentum, the dispersion relation reaches a maximum, then decreases to a minimum (corresponding to rotons), before increasing again [27, 28]. Consequently, the roton-like dispersion curve usually reverts twice with one local minimum (roton) and one local maximum (maxon), allowing for three modes (two forward modes and one backward mode) with different wavenumbers coexisting at the same frequency [27, 28]. However, the dispersion curve of the ZGV modes does not show a linear growth from zero frequency, and it reverts only once, allowing for only one backward and one forward mode with different wave numbers coexisting at the same frequency.

To understand the origin of the roton-like behaviour in acoustic metamaterials, we plot the simulated mean energy flux along the x -direction in a unit cell for three different Bloch modes at the same frequency of 1.35 kHz in figure 1(f), including two forward modes (A and C) and one backward mode (B) with different wavevectors and group velocities. For two eigenmodes with positive group velocity (A and C), the mean energy flux in both the vertical (nearest-neighbour interaction) and oblique connecting tubes (third-nearest-neighbour interaction) is positive. In sharp contrast, for eigenmode with negative group velocity (B), the mean energy flux is positive in the vertical connecting tube but is negative in the oblique connecting tubes, which supports a backward propagating wave. It is clear that the sum of the two opposite energy fluxes is negative, consistent with the negative group velocity of the dispersion relations shown in figures 1(d) and (e). The two energy fluxes moving forward and backward can give rise to a vortex-like behaviour of the energy flux, very similar to Feynman's intuitive appealing picture of rotons which correspond to some sort of stirring motions due to a 'return flow' [2].

To further elaborate the experimental results, the practical acoustic metamaterial structure can be translated to a one-dimensional (1D) toy spring-mass model with the acoustic resonator and tubes playing roles of mass and spring (see figure 1(c)), respectively. Here, the black straight lines (green arc lines) represent the nearest-neighbour interactions K_1 (the third-nearest-neighbour interactions K_3). Newton's equation of motion in this model can be written as

$$m\ddot{u} = K_1(u_{n+1} - 2u_n + u_{n-1}) + K_N(u_{n+N} - 2u_n + u_{n-N}). \quad (1)$$

where m is the mass, \ddot{u} is the acceleration of the mass displacement u_n at lattice site n , and K_N is the spring constant representing N th-nearest-neighbour interactions, with $N = 3$ in our case. The corresponding dispersion relation is

$$\omega(k) = 2\sqrt{\frac{K_1}{m}\sin^2\left(\frac{ka}{2}\right) + \frac{K_N}{m}\sin^2\left(\frac{Nka}{2}\right)}. \quad (2)$$

By fitting our measured dispersion relation to equation (2), we obtain $k_1 = 298 \text{ N m}^{-1}$, $k_3 = 454 \text{ N m}^{-1}$, and $m = 2.59 \times 10^{-5} \text{ kg}$ for our experimental sample. The fitted curve is represented by the blue dashed line in figure 1(d), which is consistent with our measured result.

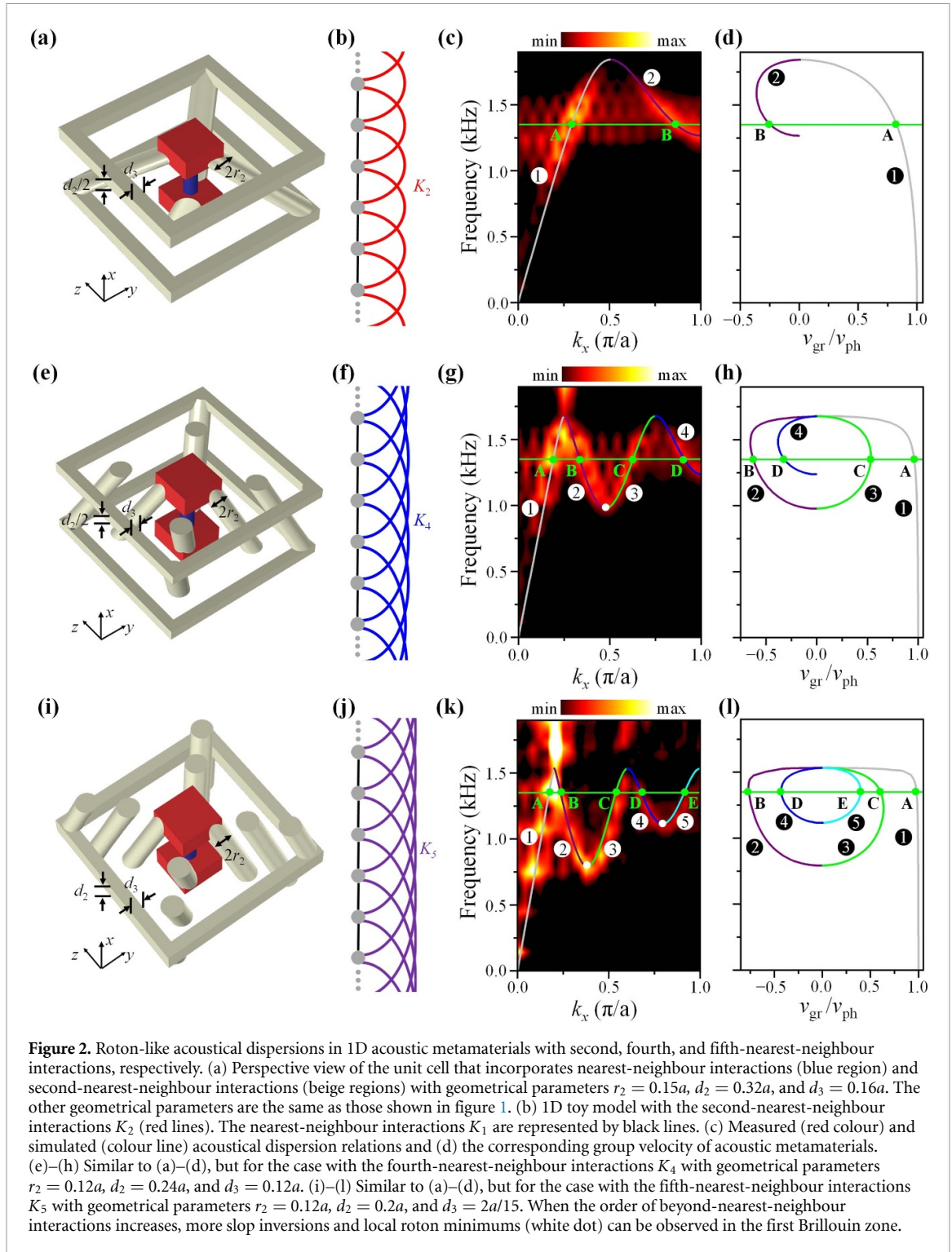
The displacement of the mass at lattice site n can be given by $u_n(t) = \tilde{u} \exp(i(kna - \omega t))$, where \tilde{u} , k and ω represent amplitude, wavenumber and angular frequency. The mean energy flow in the 1D toy model is contributed by two parts [27], is given by

$$\langle p(k) \rangle = \frac{1}{2} \tilde{u}^2 \omega (K_1 \sin(ka) + NK_N \sin(Nka)). \quad (3)$$

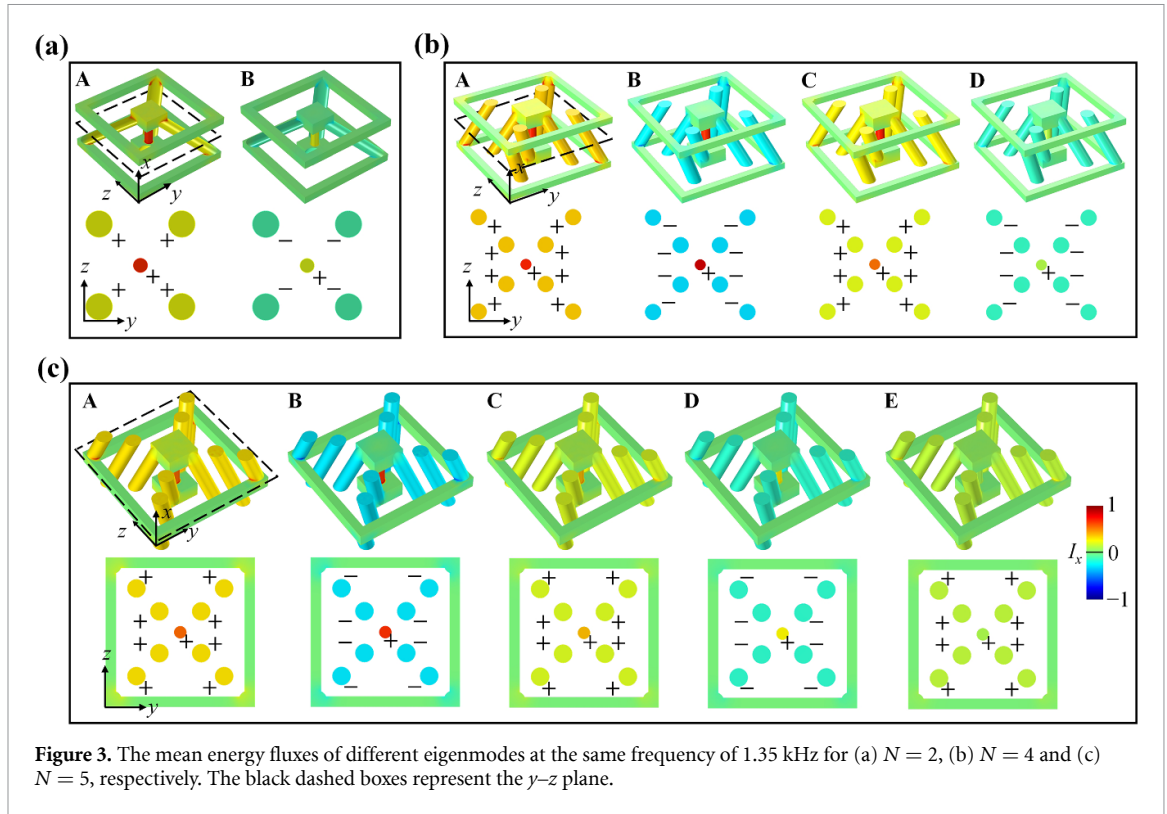
The first term is always positive for $0 < k < \pi/a$, which stems from the nearest-neighbour interactions. The second term originating from the beyond-nearest-neighbour interactions is negative in the interval $k \in [\pi/(3a), 2\pi/(3a)]$, leading to a net negative energy flow if $K_N/K_1 > 1/N$.

3.2. Multiple rotons in acoustic metamaterials with higher beyond-nearest-neighbour interaction orders

Having established the exotic features of the roton-like dispersion in nonlocal acoustic metamaterials with long-range interactions, we discuss the dispersion engineering of the nonlocal acoustic metamaterials by tuning the long-range interaction orders. It has been theoretically predicted [27] that a roton-like minimum



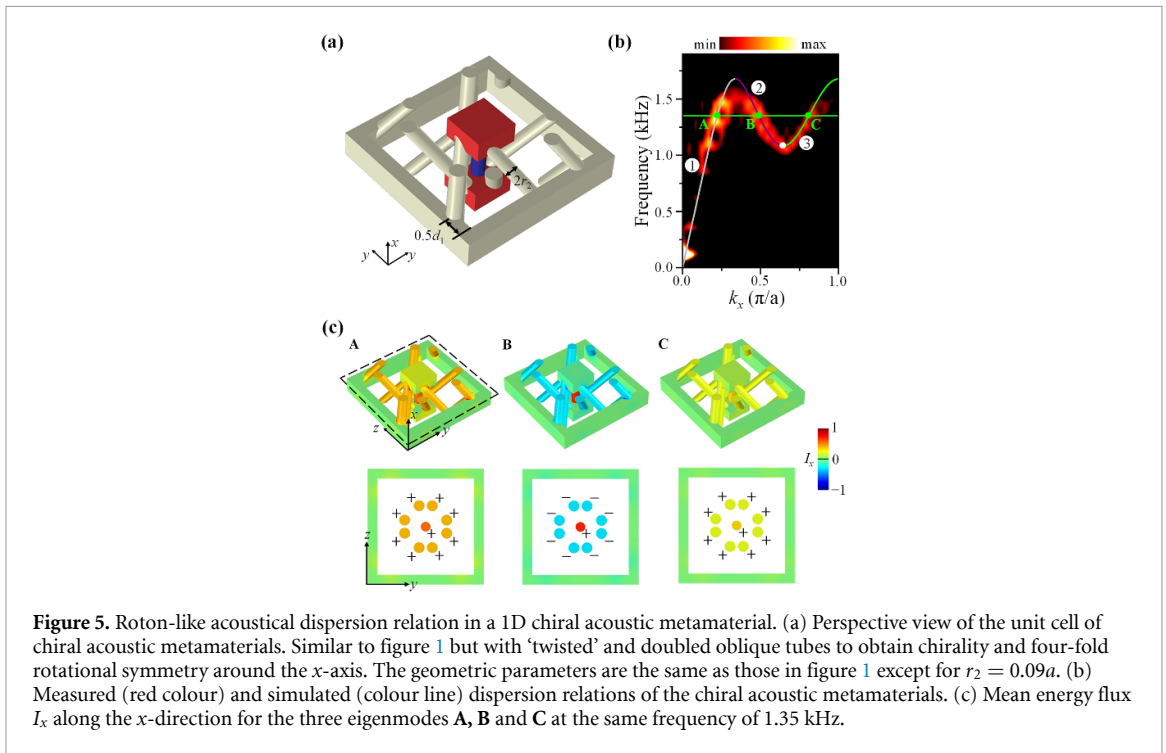
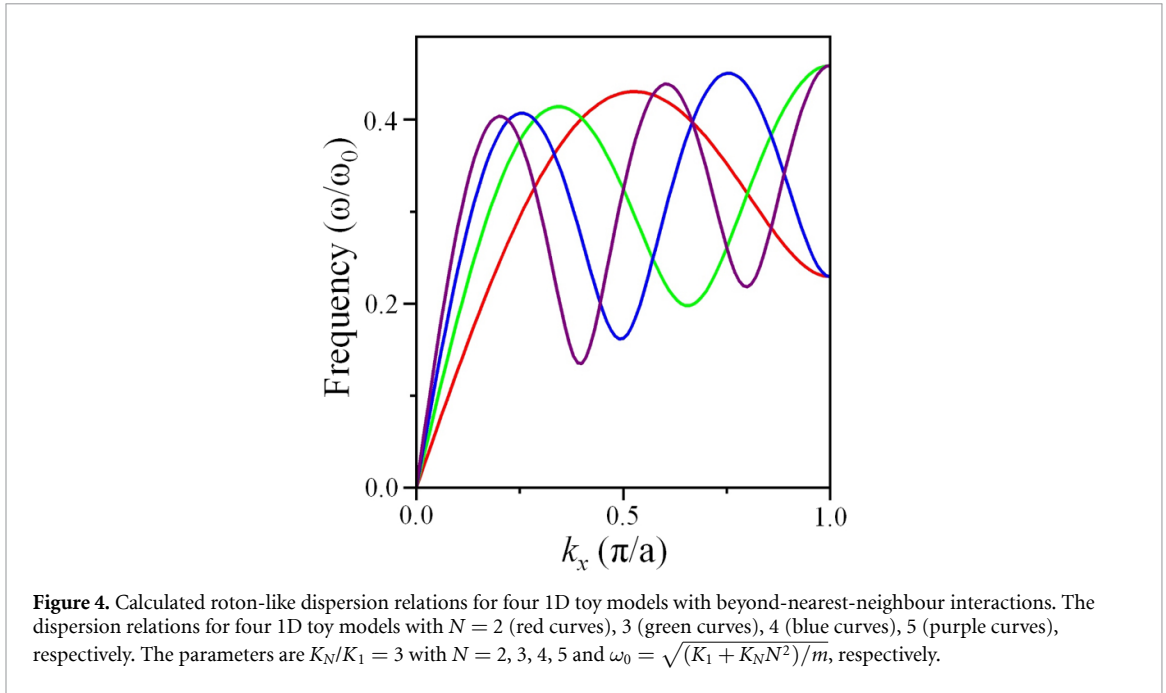
occurs if and only if the interactions order is sufficiently high (i.e. $N \geq 3$) and the strength of the beyond-nearest-neighbour interactions is sufficiently large (i.e. $K_N/K_1 > 1/N$). More remarkably, the number of roton-minimum and the negative slope region of the roton-like dispersion can be controlled by tailoring the long-range interaction order. To verify the influence of the order of beyond-nearest-neighbour interactions on the dispersion band, we design and fabricate three acoustic metamaterials with second- ($N = 2$), fourth- ($N = 4$), and fifth-nearest-neighbour ($N = 5$) interactions, respectively. Their unit cells are schematically shown in figures 2(a), (e) and (i) respectively, where the vertical cylindrical tubes (blue region) provide the nearest-neighbour interaction ($N = 1$) and the oblique cylindrical connecting tubes with the auxiliary hollow frames (beige regions) provide the second- ($N = 2$), fourth- ($N = 4$) or fifth-nearest-neighbour ($N = 5$) interactions independently.



For the case of $N = 2$, the 1D toy model with second-nearest-neighbour interactions K_2 (red arc line) is shown in figure 2(b). The measured (red colour) and calculated (colour line) band dispersions only exhibit a maxon-maximum, and its group velocity switches sign for only once, as shown in figures 2(c) and (d), respectively. In this situation, there are only two coexisting eigenmodes with different wavevectors and group velocities at the same frequency. This dispersion relation has no roton minimum and is similar to traditional metamaterial dispersion with a single negative slope region. We then study the case of $N = 4$, whose 1D toy model with the fourth-nearest-neighbour interactions K_4 (blue arc line) is shown in figure 2(f). For the case of $N = 4$, the measured (red colour) and simulated (colour line) dispersion relations are more complex with the sign of group velocity switches three times and support four different coexisting acoustic eigenmodes at one single frequency, displaying two maxon-maximums and one roton-minimum (white dot), as shown in figures 2(g) and (h), respectively. Now we continue to increase the long-range interaction order and explore another case with $N = 5$, whose 1D toy model with the fifth-nearest-neighbour interactions K_5 (purple arc line) is shown in figure 2(j). The measured (red colour) and simulated (colour line) dispersion relations reverse four times and support five different coexisting acoustic eigenmodes at one single frequency, displaying two maxon-maximums and two roton-minimums (white dots), as shown in figures 2(k) and (l), respectively. Note that the bright regions above the roton-like dispersion in figures 2(g) and (k) come from a higher band. The mean energy fluxes of different coexisting eigenmodes at the same frequency of 1.35 kHz for $N = 2, 4$ and 5 are shown in figure 3. Both the measured and simulated results reveal, as expected, roton behaviour occurs only for beyond-nearest-neighbour interaction order $N \geq 3$ and more slope inversions, and roton minimums can be brought into the first Brillouin zone by increasing the long-range interaction order. Note that multiple classical rotons on a single dispersion curve achieved when $N \geq 5$ have never been theoretically proposed and experimentally demonstrated in both the quantum and classical-wave systems before. Theoretically derived roton-like dispersion relations for four 1D toy models with different orders of long-range interactions are shown in figure 4.

3.3. Roton-like dispersion relation in a chiral acoustic metamaterial

Recently, it has been theoretically reported that the roton-like dispersion relations for transverse acoustical elastic waves can be realized in noncentrosymmetric micropolar crystal based on chiral micropolar elasticity theory, where chirality is a necessary condition for roton-like behaviours [32]. Hence, it is natural to ask whether chirality plays an important role in the roton-like behaviours in our airborne acoustic system. Here, we introduce chirality into our acoustic metamaterials with $N = 3$ by twisting and doubling the oblique connecting tubes to construct an acoustic metamaterial with four-fold rotational symmetry around the



x -axis, whose unit cell is schematically shown in figure 5(a). As both the inversion and mirror symmetries are absent, the newly designed acoustic metamaterial is structurally chiral. Interestingly, both the measured (red colour) and simulated (colour line) dispersion relations of the chiral acoustic metamaterial (figure 5(b)) display a roton-like behaviour which is very similar to that of the achiral acoustic metamaterials in figure 1(d). The energy flux of the three coexisting modes shown in figure 5(c) further confirmed the similarity between the chiral and achiral acoustic metamaterials with beyond-nearest-neighbour interactions. Therefore, we have experimentally verified that both the chiral and achiral acoustic metamaterials with beyond-nearest-neighbour interactions can support roton-like dispersion relations with similar properties.

3.4. Multidirectional roton-like dispersion relations in a 2D nonlocal acoustic metamaterial

We have also theoretically proposed and experimentally realized multidirectional roton-like dispersion relations in a 2D nonlocal acoustic metamaterial with third-nearest-neighbour interactions in both

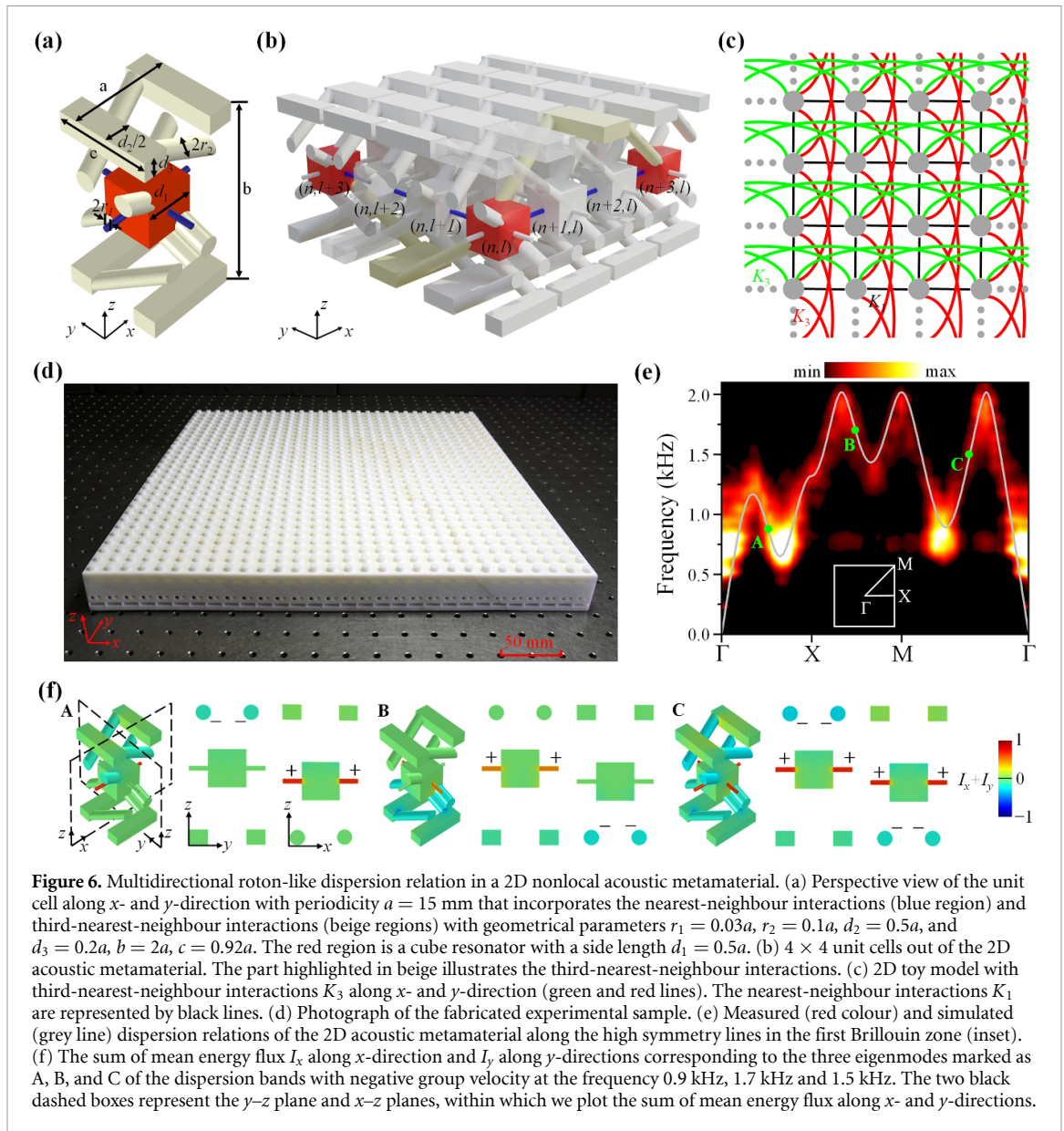
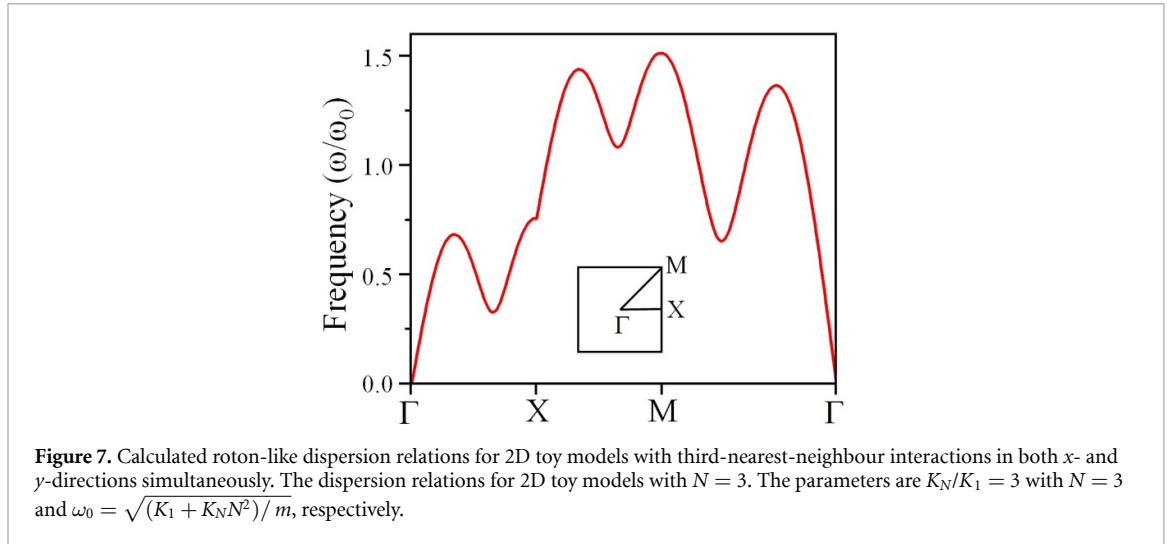


Figure 6. Multidirectional roton-like dispersion relation in a 2D nonlocal acoustic metamaterial. (a) Perspective view of the unit cell along x - and y -direction with periodicity $a = 15$ mm that incorporates the nearest-neighbour interactions (blue region) and third-nearest-neighbour interactions (beige regions) with geometrical parameters $r_1 = 0.03a$, $r_2 = 0.1a$, $d_2 = 0.5a$, and $d_3 = 0.2a$, $b = 2a$, $c = 0.92a$. The red region is a cube resonator with a side length $d_1 = 0.5a$. (b) 4×4 unit cells out of the 2D acoustic metamaterial. The part highlighted in beige illustrates the third-nearest-neighbour interactions. (c) 2D toy model with third-nearest-neighbour interactions K_3 along x - and y -direction (green and red lines). The nearest-neighbour interactions K_1 are represented by black lines. (d) Photograph of the fabricated experimental sample. (e) Measured (red colour) and simulated (grey line) dispersion relations of the 2D acoustic metamaterial along the high symmetry lines in the first Brillouin zone (inset). (f) The sum of mean energy flux I_x along x -direction and I_y along y -directions corresponding to the three eigenmodes marked as A, B, and C of the dispersion bands with negative group velocity at the frequency 0.9 kHz, 1.7 kHz and 1.5 kHz. The two black dashed boxes represent the y - z plane and x - z planes, within which we plot the sum of mean energy flux along x - and y -directions.

horizontal (x) and vertical (y) directions. Since the long-range interactions in the 2D system are far more complex than the 1D case, we propose a completely different architecture to construct the 2D nonlocal acoustic metamaterial with long-range interactions. The unit cell of the 2D acoustic metamaterial is schematically shown in figure 6(a); the original ancillary hollow frame mediating the third-nearest-neighbour interactions in 1D acoustic metamaterials is reduced to four hollow rectangular tubes to construct the third-nearest-neighbour interactions in two orthogonal directions. A perspective view of 4×4 unit cells out of a corresponding 2D nonlocal acoustic metamaterial is shown in figure 6(b) for clarity. The part highlighted in beige illustrates the third-nearest-neighbour interactions in two orthogonal directions. In the x (y) direction, one circular coupling tube connects the first cube (n, l) to the upper (lower) ancillary rectangular box and the other circular coupling tube connects this ancillary rectangular box to the fourth cube $(n + 3, l)$ ($n, l + 3$), which has a distance of $3a$ with respect to the first cube in both directions. The 2D toy model with equal third-nearest-neighbour interactions along x - and y -directions (green and red lines) is depicted in figure 6(c). Equation of motion in this model can be written as

$$\begin{aligned}
 m\ddot{u}_{xy} = & K_1 \left[\left(u_{(n+1,l)}^x - 2u_{(n,l)}^x + u_{(n-1,l)}^x \right) + \left(u_{(n,l+1)}^y - 2u_{(n,l)}^y + u_{(n,l-1)}^y \right) \right] \\
 & + K_N \left[\left(u_{(n+N,l)}^x - 2u_{(n,l)}^x + u_{(n-N,l)}^x \right) + \left(u_{(n,l+N)}^y - 2u_{(n,l)}^y + u_{(n,l-N)}^y \right) \right]. \quad (4)
 \end{aligned}$$



where m is the mass, \ddot{u}_{xy} is the acceleration of the mass displacement $u_{(n,l)}^x$ and $u_{(n,l)}^y$ at lattice site (n,l) , and K_N is the spring constant representing N th-nearest-neighbour interactions, with $N = 3$ in our case. The solution of this equation of motion are Bloch waves in both x - and y -directions, following the theoretical dispersion relation of this 2D toy model:

$$\omega(k_x, k_y) = 2 \sqrt{\frac{K_1}{m} \left[\sin^2\left(\frac{k_x a}{2}\right) + \sin^2\left(\frac{k_y a}{2}\right) \right] + \frac{K_N}{m} \left[\sin^2\left(\frac{Nk_x a}{2}\right) + \sin^2\left(\frac{Nk_y a}{2}\right) \right]}. \quad (5)$$

The theoretically derived dispersion relations of the 2D toy model with third-nearest-neighbour interactions are depicted in figure 7. We then fabricate the 2D acoustic metamaterial (see the photograph of the experimental sample in figure 6(d)) and measure its dispersion relations. The measured (red colour) and simulated (grey line) dispersion relations are shown in figure 6(e), exhibiting multidirectional roton-like dispersion relation at high-symmetry lines. In figure 6(f), we plot the sum of mean energy flux along x and y directions corresponding to the three eigenmodes marked as A, B, and C of the dispersion bands with negative group velocity in figure 6(e). For modes A and B, the sum of mean energy flux in two directions is positive in the nearest-neighbour connecting tube along x - or y -direction, but is negative in the upper or lower third-nearest-neighbour oblique connecting tubes. For mode C, the sum of mean energy flux in two directions is positive both in the nearest-neighbour connecting tube along x - and y -directions, but is negative both in the upper and lower third-nearest-neighbour oblique connecting tubes. This unconventional feature of energy fluxes flow gives rise to a vortex-like behaviour of acoustic waves in multiple directions.

4. Conclusion and discussion

In conclusion, we have designed and experimentally demonstrated the long-sought roton-like dispersion relations in nonlocal acoustic metamaterials with beyond-nearest-neighbour interactions. With increasing the order of beyond-nearest-neighbour interactions, multiple slope inversions and classical rotons can be achieved on a single dispersion band with no quantum equivalent. By introducing long-range coupling in both horizontal (x) and vertical (y) directions, multidirectional roton-like dispersion relations can be realized in 2D nonlocal acoustic metamaterials. Moreover, we also experimentally verify that both chiral and achiral acoustic metamaterials with long-range interactions can support roton-like dispersions. The realization of roton-like dispersions opens up multiple avenues for explorations of metamaterials, including broadband negative refractive index media and nonlocal metamaterials with arbitrary dispersion relations. Our work points to a direction beyond the nearest-neighbour interactions between the constituent elements of a physical system, and offers a powerful platform to engineer the dispersion relations that could enable the observation of unusual physical phenomena and the abundant applications beyond traditional negative-index metamaterials. Although demonstrated in acoustic metamaterials, the same principle can be extended to other classical-wave systems such as photonics, plasmonic, and mechanical systems.

Data availability statement

The data that support the findings of this study are available upon reasonable request from the authors.

Acknowledgments

Z.G. acknowledge support from the National Natural Science Foundation of China under grant number 12104211, 6101020101, SUSTech Start-up Grant (Y01236148, Y01236248). The work at Zhejiang University was sponsored by the Key Research and Development Program of the Ministry of Science and Technology under Grants No. 2022YFA1404902 (Y Y) and No.2022YFA1405201 (Y Y), the National Natural Science Foundation of China (NNSFC) under Grants No. 62175215 (Y Y), the Fundamental Research Funds for the Central Universities (2021FZZX001-19) (Y Y), and the Excellent Young Scientists Fund Program (Overseas) of China (Y Y). H S acknowledged the support of the National Natural Science Foundation of China (Grant Nos. 12274183 and 12174159), and the State Key Laboratory of Acoustics, Chinese Academy of Science under Grant No. SKLA202216.

Author contributions

Y Y and Z G initiated the project. Z Z designed the structures and did the numerical simulations with help from G L and X X Z G Z Z, H S, Y B, and F C fabricated the samples. H S and Y G performed the measurements. Z Z, Z G and Y Y analysed the data and wrote the manuscript. P S helped to revise the manuscript. Z G and Y Y supervised the project.

Conflict of interest

The authors declare no competing interests.

ORCID iD

Hong-xiang Sun  <https://orcid.org/0000-0003-4646-6837>

References

- [1] Landau L 1941 *Phys. Rev.* **60** 356
- [2] Feynman R P and Cohen M 1956 *Phys. Rev.* **102** 1189
- [3] Feynman R P 1957 *Rev. Mod. Phys.* **29** 205
- [4] Henshaw D G and Woods A D B 1961 *Phys. Rev. Lett.* **121** 1266
- [5] Woods A D B 1965 *Phys. Rev. Lett.* **14** 355
- [6] Beauvois K, Dawidowski J, Fåk B, Godfrin H, Krotscheck E, Ollivier J and Sultan A 2018 *Phys. Rev. B* **97** 184520
- [7] Godfrin H, Beauvois K, Sultan A, Krotscheck E, Dawidowski J, Fåk B and Ollivier J 2021 *Phys. Rev. B* **103** 104516
- [8] Stone M B, Zaliznyak I A, Hong T, Broholm C L and Reich D H 2006 *Nature* **440** 187
- [9] Kukushkin I V, Smet J H, Scarola V W, Umansky V and Klitzing K V 2009 *Science* **324** 1044
- [10] Godfrin H, Meschke M, Lauter H J, Sultan A, Böhm H M, Krotscheck E and Panholzer M 2012 *Nature* **483** 576
- [11] Mottl R, Brennecke F, Baumann K, Landig R, Donner T and Esslinger T 2012 *Science* **336** 1570
- [12] Chomaz L, van Bijnen R M W, Petter D, Faraoni G, Baier S, Becher J H, Mark M J, Wächtler F, Santos L and Ferlaino F 2018 *Nat. Phys.* **14** 442
- [13] Cummer S A, Christensen J and Alù A 2016 *Nat. Rev. Mater.* **1** 16001
- [14] Fang N, Xi D, Xu J, Ambati M, Srituravanich W, Sun C and Zhang X 2006 *Nat. Mater.* **5** 452
- [15] Brunet T, Merlin A, Mascaro B, Zimny K, Leng J, Poncelet O, Aristégui C and Mondain-Monva O 2015 *Nat. Mater.* **14** 384
- [16] Kaina N, Lemoult F, Fink M and Lerosey G 2015 *Nature* **525** 77
- [17] Li J, Fok L, Yim X, Bartal G and Zhang X 2009 *Nat. Mater.* **8** 931
- [18] Zhu J, Christensen J, Jung J, Martin-Moreno L, Yin X, Fok L, Zhang X and Garcia-Vidal F J 2011 *Nat. Phys.* **7** 52
- [19] Zhang S, Xia C and Fang N 2011 *Phys. Rev. Lett.* **106** 024301
- [20] Zigoneanu L, Popa B-I and Cummer S A 2014 *Nat. Mater.* **13** 352
- [21] Yang Z, Gao F, Shi X, Shi X, Lin X, Gao Z, Chong Y and Zhang B 2015 *Phys. Rev. Lett.* **114** 114301
- [22] He C, Ni X, Ge H, Sun X, Chen Y, Lu M and Liu X 2016 *Nat. Phys.* **12** 1124
- [23] Lu J, Qiu C, Ye L, Fan X, Ke M, Zhang F and Liu Z 2017 *Nat. Phys.* **13** 369
- [24] Li F, Huang X, Lu J, Ma J and Liu Z 2018 *Nat. Phys.* **14** 30
- [25] He H, Qiu C, Ye L, Cai X, Fan X, Ke M, Zhang F and Liu Z 2018 *Nature* **560** 61
- [26] Yang Y, Sun H, Xia J, Xue H, Gao Z, Ge Y, Jia D, Yuan S and Zhang B 2019 *Nat. Phys.* **15** 645
- [27] Chen Y, Kadic M and Wegener M 2021 *Nat. Commun.* **12** 3278
- [28] Fleury R 2021 *Nat. Phys.* **17** 766
- [29] Smith D R, Pendry J B and Wiltshire M 2004 *Science* **305** 788
- [30] Prada C, Clorennec D and Royer D 2008 *J. Acoust. Soc. Am.* **124** 1
- [31] Caliendo C and Hamidullah M 2017 *J. Phys. D: Appl. Phys.* **50** 474002
- [32] Kishine J, Ovchinnikov A S and Tereshchenko A 2020 *Phys. Rev. Lett.* **125** 245302